Charge-Induced Force Noise on Free-Falling Test Masses: Results from LISA Pathfinder

Armano, M ; Audley, H ; Auger, G ; Baird, J T ; Binetruy, P ; Born, M ; Bortoluzzi, D ; Brandt, N ; Bursi, A ; Caleno, M ; Cavalleri, A ; Cesarini, A ; Cruise, M ; Danzmann, K ; de Deus Silva, M ; Diepholz, I ; Dolesi, R ; Dunbar, N ; Ferraioli, L ; Ferroni, V ; Fitzsimons, E D ; Flatscher, R ; Freschi, M ; Gallegos, J ; García Marirrodriga, C ; Gerndt, R ; Gesa, L ; Gibert, F ; Giardini, D ; Giusteri, R ; et al

DOI: https://doi.org/10.1103/PhysRevLett.118.171101

Charge-Induced Force Noise on Free-Falling Test Masses: Results from LISA Pathfinder

M. Armano,[1] H. Audley,[2] G. Auger,[3] J. T. Baird,[4] P. Binetruy,[3,†] M. Born,[2] D. Bortoluzzi,[5] N. Brandt,[6] A. Bursi,[7] M. Caleno,[8] A. Cavalleri,[9] A. Cesarini,[9] M. Cruise,[10] K. Danzmann,[2] M. de Deus Silva,[1] I. Diepholz,[2] R. Dolesi,[9] N. Dunbar,[11] L. Ferraioli,[12] V. Ferroni,[9] E. D. Fitzsimons,[13] R. Flatscher,[6] M. Freschi,[1] J. Gallegos,[1] C. García Marirrodriga,[8] R. Gerndt,[6] L. Gesa,[14] F. Gibert,[9] D. Giardini,[12] R. Giusteri,[9] C. Grimani,[15] J. Grzymisch,[8] I. Harrison,[16] G. Heinzel,[2] M. Hewitson,[2] D. Hollington,[4] M. Hueller,[9] J. Huesler,[8] H. Inchauspé,[3,‡] O. Jennrich,[8] P. Jetzer,[17] B. Johlander,[8] N. Karnesis,[2] B. Kaune,[2] C. J. Killow,[18] N. Korsakova,[18] I. Lloro,[14] L. Liu,[9] J. P. López-Zaragoza,[14] R. Maarschalkerweerd,[16] S. Madden,[8] D. Mance,[12] V. Martín,[14] L. Martin-Polo,[1] J. Martino,[3] F. Martin-Porqueras,[1] I. Mateos,[14] P. W. McNamara,[8] J. Mendes,[16] L. Mendes,[1] A. Moroni,[7] M. Nofrarias,[14] S. Paczkowski,[2] M. Perreur-Lloyd,[18] A. Petiteau,[3] P. Pivato,[9] E. Plagnol,[3] P. Prat,[3] U. Ragnit,[8] J. Ramos-Castro,[19,20] J. Reiche,[2] J. A. Romera Perez,[8] D. I. Robertson,[18] H. Rozemeijer,[8] F. Rivas,[14] G. Russano,[9] P. Sarra,[7] A. Schleicher,[6] J. Slutsky,[21] C. Sopuerta,[14] T. J. Sumner,[4] D. Texier,[1] J. I. Thorpe,[21] C. Trenkel,[11] D. Vetrugno,[9] S. Vitale,[9] G. Wanner,[2] H. Ward,[18] P. J. Wass,[4,*] D. Wealthy,[11] W. J. Weber,[9] A. Wittchen,[2] C. Zanoni,[5] T. Ziegler,[6] and P. Zweifel[12]

(LISA Pathfinder Collaboration)

[1]*European Space Astronomy Centre, European Space Agency, Villanueva de la Cañada, 28692 Madrid, Spain*
[2]*Albert-Einstein-Institut, Max-Planck-Institut für Gravitationsphysik und Universität Hannover, 30167 Hannover, Germany*
[3]*APC UMR7164, Université Paris Diderot, 10, rue Alice Domon et Léonie Duquet, 75205 Paris Cedex 13, France*
[4]*High Energy Physics Group, Department of Physics, Imperial College London, Blackett Laboratory, Prince Consort Road, London SW7 2BW, United Kingdom*
[5]*Department of Industrial Engineering, University of Trento, via Sommarive 9, 38123 Trento, Italy and Trento Institute for Fundamental Physics and Application/INFN, Italy*
[6]*Airbus Defence and Space, Claude-Dornier-Strasse, 88090 Immenstaad, Germany*
[7]*CGS S.p.A, Compagnia Generale per lo Spazio, Via Gallarate, 150-20151 Milano, Italy*
[8]*European Space Technology Centre, European Space Agency, Keplerlaan 1, 2200 AG Noordwijk, Netherlands*
[9]*Dipartimento di Fisica, Università di Trento and Trento Institute for Fundamental Physics and Application/INFN, 38123 Povo, Trento, Italy*
[10]*Department of Physics and Astronomy, University of Birmingham, Birmingham, Edgbaston Park Road, Birmingham B15 2TT, United Kingdom*
[11]*Airbus Defence and Space, Gunnels Wood Road, Stevenage, Hertfordshire SG1 2AS, United Kingdom*
[12]*Institut für Geophysik, ETH Zürich, Sonneggstrasse 5, CH-8092, Zürich, Switzerland*
[13]*United Kingdom Astronomy Technology Centre, Royal Observatory, Edinburgh EH9 3HJ, United Kingdom*
[14]*Institut de Ciències de l'Espai (CSIC-IEEC), Campus UAB, Carrer de Can Magrans s/n, 08193 Cerdanyola del Vallès, Spain*
[15]*DiSPeA, Università di Urbino "Carlo Bo", Via S. Chiara, 27 61029 Urbino/INFN, Italy*
[16]*European Space Operations Centre, European Space Agency, 64293 Darmstadt, Germany*
[17]*Physik Institut, Universität Zürich, Winterthurerstrasse 190, CH-8057 Zürich, Switzerland*
[18]*SUPA, Institute for Gravitational Research, School of Physics and Astronomy, University of Glasgow, Glasgow G12 8QQ, United Kingdom*
[19]*Department d'Enginyeria Electrònica, Universitat Politècnica de Catalunya, 08034 Barcelona, Spain*
[20]*Institut d'Estudis Espacials de Catalunya (IEEC), C/ Gran Capità 2-4, 08034 Barcelona, Spain*
[21]*NASA Goddard Space Flight Center, 8800 Greenbelt Road, Greenbelt, Maryland 20771, USA*

(Received 16 February 2017; published 26 April 2017)

We report on electrostatic measurements made on board the European Space Agency mission LISA Pathfinder. Detailed measurements of the charge-induced electrostatic forces exerted on free-falling test masses (TMs) inside the capacitive gravitational reference sensor are the first made in a relevant environment for a space-based gravitational wave detector. Employing a combination of charge control and electric-field compensation, we show that the level of charge-induced acceleration noise on a single TM can be maintained at a level close to 1.0 $\mathrm{fm\,s^{-2}\,Hz^{-1/2}}$ across the 0.1–100 mHz frequency band that is crucial to an observatory such as the Laser Interferometer Space Antenna (LISA). Using dedicated measurements that detect these effects in the differential acceleration between the two test masses, we resolve the stochastic nature of the TM charge buildup due to interplanetary cosmic rays and the TM charge-to-force coupling through stray

electric fields in the sensor. All our measurements are in good agreement with predictions based on a relatively simple electrostatic model of the LISA Pathfinder instrument.

DOI: 10.1103/PhysRevLett.118.171101

Introduction.—Sensitive gravitational experiments employ quasi-free-falling isolated test masses (TMs) as a reference system for the measurement of the local curvature of space-time. Electrostatic free charge and stray potentials introduce unwanted disturbances that can limit measurement precision. The effect is relevant for gravitational wave (GW) observatories both in space [1,2] and on-ground [3] tests of the equivalence principal [4] and measurements of relativistic effects on precessing gyroscopes [5].

The Laser Interferometer Space Antenna (LISA) Pathfinder spacecraft [6], a technology-demonstration experiment for a space-based gravitational wave observatory, LISA [7,8], was launched on December 3, 2015. The aim of the mission was to demonstrate the ability to fly free-falling test masses in a single spacecraft with a differential acceleration noise below 30 $\mathrm{fm\,s^{-2}\,Hz^{-1/2}}$ above 1 mHz. The sensitivity of the instrument has far exceeded its design specification, achieving a level close to the LISA goal from 0.1–100 mHz and around 5 $\mathrm{fm\,s^{-2}\,Hz^{-1/2}}$ in the mHz band [9]. In this Letter, we describe the measurements and techniques used to minimize charge-related electrostatic forces and evaluate their contribution to the differential acceleration noise of the test masses.

The LISA Pathfinder test masses, identical to those for LISA, are 46-mm cubes of mass 1.928 kg made from a gold-platinum alloy. They sit within a 6 degree-of-freedom capacitive position sensor and actuator, the gravitational reference sensor (GRS) [10,11]. The masses are separated from the walls of the sensor by gaps of between 2.9 and 4 mm and have no grounding wire. All test mass and sensor surfaces are gold coated. The large gaps mitigate the impact of surface forces [12] and the absence of a grounding wire eliminates thermal noise associated with mechanical damping that dominates the low-frequency performance of accelerometers in existing geodesy and fundamental physics missions [13–15].

The achieved level of sensitivity to the differential acceleration of the test masses is made possible by an additional high-precision readout along their common x axis provided by a laser interferometer [16–18]. The measurement noise in the differential test mass position, measured above 60 mHz, is 35 $\mathrm{fm\,Hz^{-1/2}}$ [9].

The GRS consists of a system of 12 electrodes for TM position sensing and actuation, and a further six for capacitive biasing of the test mass at 100 kHz. Actuation is achieved with audio-frequency sinusoidal voltages. dc or slowly varying ($f \sim$ mHz) voltage signals can be applied to measure TM charge, and balance stray electrostatic fields, as will be discussed shortly. Voltages on all electrodes originate from the GRS front-end electronics [19].

High-energy cosmic rays and solar energetic particles, mostly protons, penetrate the spacecraft and instrument shielding depositing charge on the test mass, either by stopping directly or by secondary emission [20–24]. Limiting charge accumulation on the electrically isolated TMs is needed to control electrostatic forces, the subject of this Letter. In LISA Pathfinder, noncontact discharge is achieved by illuminating the sensor and test-mass surfaces with UV light and transferring charge by photoemission [25] in a similar way to that already demonstrated on Gravity Probe-B [26]. A detailed account of the performance of the LISA Pathfinder UV discharge system will be provided in a subsequent article.

Description of the problem and experimental techniques.—As well as providing desired actuation forces, the GRS is a source of unwanted electrostatic disturbances on the test mass [11,27]. With the TM centered, the dominant source of electrostatic force noise is the interaction between the TM charge, q, and stray electric fields. We represent these by an effective potential difference between opposite sides of the TM, Δ_x, the equivalent uniform single GRS x-electrode potential that would give the same average stray field along the x axis. The resulting force along the x axis, following the notation of [2], is

$$F_x(q) = -\frac{q}{C_\mathrm{T}}\left|\frac{\partial C_x}{\partial x}\right|\Delta_x, \tag{1}$$

where $\partial C_x/\partial x$ is the derivative of a single sensing electrode capacitance with respect to TM displacement along x, and C_T is the total capacitance of the test mass with respect to the GRS. Finite element modeling calculates $C_\mathrm{T} = 34.2$ pF and $\partial C_x/\partial x = 291\ \mathrm{pF\,m^{-1}}$.

In LISA Pathfinder, the principle science observable is the differential force per unit mass acting on the two TMs, $\Delta g \equiv F_{2x}/m_2 - F_{1x}/m_1$. Thus, the measurement is sensitive to the in-band fluctuations of both Δ_x and q for the two TMs. Force noise is produced by a nonzero charge q, coupling with fluctuations in the average potential difference Δ_x and, likewise, stochastic charge fluctuations mixing with any nonzero potential difference. We measure these effects with a number of dedicated techniques.

The test-mass charge, q can be detected in its effect on the TM potential, $\delta V_\mathrm{TM} = \delta q/C_T$, measured by applying sinusoidally varying voltages with amplitude V_MOD and frequency, f_MOD on the x-axis electrodes, a technique well demonstrated in ground-based investigations [28,29]. The resulting force on the TM is $F_x(f_\mathrm{MOD}) = -4|\partial C_x/\partial x|V_\mathrm{MOD}V_\mathrm{TM}$. A continuous measurement provides an extended time series

of $q(t)$ from which the low-frequency behavior of the charge buildup can be studied.

To measure the relevant stray potential difference Δ_x, we introduce a compensating potential $\pm V_{\mathrm{COMP}}$ to each x electrode. Following the method described in [2], it is possible to estimate $\partial F_x/\partial q$ as a function of V_{COMP} measuring the change in Δg as the charge of one test mass is increased in steps by photoemission under UV illumination. By choosing a value for V_{COMP} that provides an equal and opposite potential difference to Δ_x, we can cancel dF_x/dq to first order.

The LISA Pathfinder sensitivity is sufficient that the effects of in-band fluctuations of q and Δ_x, described by their power spectral densities (PSDs), S_q and S_{Δ_x} are measurable directly in Δg by exaggerating Δ_x or q, respectively.

Simulations and ground-based laboratory measurements provide indications of the expected behavior of the test mass charge and stray potentials. High-energy physics simulations [21,22] predict a net positive charging rate of 40–70 elementary charges per second ($e\mathrm{s}^{-1}$) from galactic cosmic rays (GCRs) at the minimum of the 11-year solar activity cycle (20–40 $e\mathrm{s}^{-1}$ at maximum when GCR flux is suppressed). The associated charging-current shot noise, made up of charge transfer to and from the test mass, is equivalent to that produced by a rate of single charges, λ_{eff}, of 200–400 s^{-1}. The amplitude spectral density (ASD) of the test-mass charge has the form $S_q^{1/2} = e\sqrt{2\lambda_{\mathrm{eff}}}/2\pi f$ with an expected amplitude of 0.6–0.7 $\mathrm{fC\,Hz^{-1/2}}$ at 1 mHz.

Δ_x originates both from surface patch potentials within the sensor and the GRS electronics. Measurements with representative systems in laboratory tests have found static levels of up to 100 mV [2,30–32]. Tests on a representative electronics unit measured $S_{\Delta_x}^{1/2}$ coming from electrode-voltage fluctuations to be 30 $\mu\mathrm{V\,Hz^{-1/2}}$ at 1 mHz [19]. Tests on the real system before launch found similar levels. Torsion pendulum measurements using a representative TM and GRS and similar electronics have placed 2-σ upper limits on the total fluctuations, including patch potentials of 80 $\mu\mathrm{V\,Hz^{-1/2}}$ at 1 mHz and 290 $\mu\mathrm{V\,Hz^{-1/2}}$ at 0.1 mHz [2].

Experimental results.—A $\sim$ 3-day measurement of q was made injecting $V_{\mathrm{MOD}} = 3$ V at $f_{\mathrm{MOD}} = 6$ and 9 mHz on TM 1 and TM 2, respectively. The charge was calculated by heterodyne demodulation of Δg, with the applied V_{MOD} as the phase reference.

The average charging rates were $+22.9\ e\mathrm{s}^{-1}$ and $+24.5\ e\mathrm{s}^{-1}$ on TM 1 and TM 2, respectively. Over 10 000-s periods, the charge rate is observed to vary by $\pm 2\ e\mathrm{s}^{-1}$, caused by a combination of low frequency noise and drift. The fluctuations around the mean charging rates are shown in the lower-left panel of Fig. 1; two $> 5\sigma$ glitches in the TM 2 charge fluctuations have been removed. S_q was calculated with the Welch method, averaging 11 detrended, 40 000-s Blackman-Harris (BH) spectral windows with 50% overlap. A f^{-2} fit was applied to the PSDs, down sampled by a factor of 4 to remove data correlated by spectral windowing. The resulting ASDs are shown in the upper left panel of Fig. 1 and a summary of the results is given in Table I.

The f^{-2} dependence of the charge PSD and observed absence of correlation in the two charge time series are consistent with the model of independent Poissonian

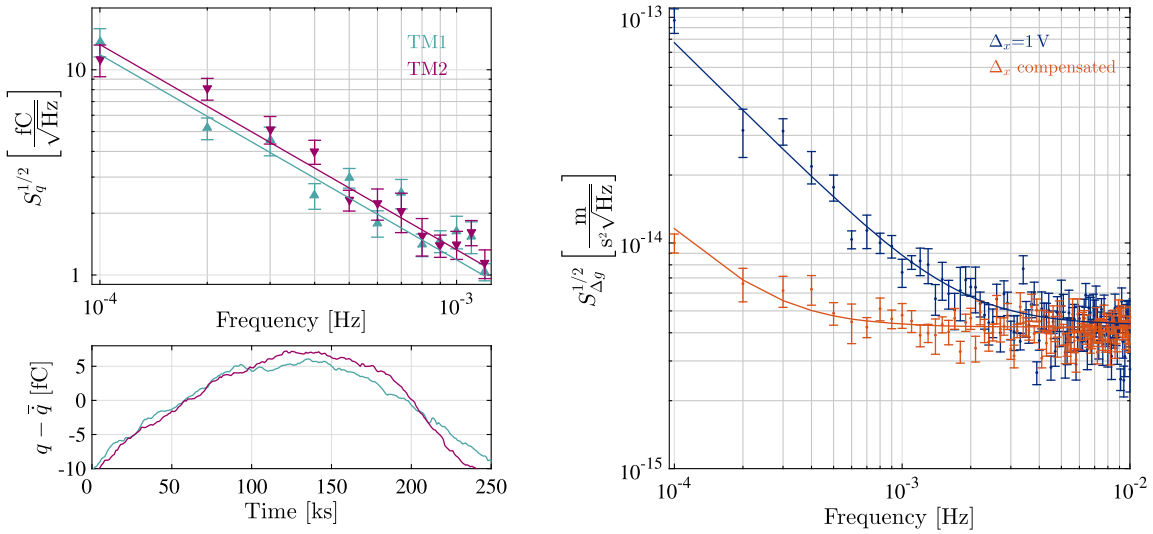

FIG. 1. Measurements of TM charge fluctuations. Upper-left: The ASD of the charge on TM 1 (upward triangle) and TM 2 (downward triangle) in the LISA band with $1/f$ fits (reduced $\chi^2 = 1.5$ and 0.9). Lower-left: The charge time series after removal of the linear trend due to the average charge rate over the course of the three-day measurement. Right: Consecutive measurements of the ASD of Δg with exaggerated Δ_x (dark-blue indicators) and with Δ_x compensated to $\lesssim 3$ mV (red indicators). Continuous curves show the result of a combined fit to the background noise and Δ_x-dependent $1/f$ excess (reduced $\chi^2 = 1.2$).

TABLE I. Test mass charging properties.

	TM1	TM2	
$\dot{q}$	$+22.9$	$+24.5$	$e\,\mathrm{s}^{-1}$
λ_{eff}	1060 ± 90	1360 ± 130	s^{-1}
$\lambda_{\mathrm{eff}(1+2)}$ [a]	2200 ± 260		s^{-1}

[a]Determined from fit to Δg with $\Delta_x = 1$ V.

processes for the two TMs, at least down to 0.1 mHz. A common drift in the charge rate at very-low frequency (visible in the time series as a quadratic dependence after removal of the linear trends due to the average charging rates) correlates well with measurements in the on-board particle monitor and is, therefore, likely caused by changes in the incident particle flux. The measured charge-noise levels have roughly 5 times the expected noise power, with effective charge rates between 1000 and 1400 s^{-1}. Possible causes for an excess are a larger-than-expected number of high-multiplicity charging events produced by very-high energy (∼TeV) cosmic rays, or a large population of low-energy (∼eV) secondaries emitted from TM and GRS surfaces. These two energy regimes are the source of most uncertainty in the charging predictions [21].

In this measurement, made some 3–4 years before solar minimum, we find test-mass charging rates within the expected range but measurably different on the two TMs. The difference in the charge rates may originate in the different volt-scale ac electrostatic fields used for force actuation in the two GRSs. If confirmed, this would favor secondary electrons as the source of excess noise. Further measurements characterizing the charge-rate behavior in detail will be the subject of future work.

The spectral density of the charge noise can also be determined from a measurement of Δg with an exaggerated potential difference Δ_x. The right panel of Fig. 1 shows two measurements of the ASD of Δg calculated with the same method described for S_q, the first lasting ∼2.5 days with $\Delta_{x_1} = \Delta_{x_2} = 1$ V and calculated by averaging nine overlapping, 40 000-s BH windows, the second ∼1 day later with both Δ_x compensated to $\lesssim 3$ mV (as described below) using 15 windows covering nearly four days. We perform a combined fit to the spectra in the frequency range $0.1 \leq f \leq 20$ mHz assuming a stationary background and an excess due to random charging proportional to Δ_x. We find the excess noise in Δg in the presence of the applied electric field is compatible with a total effective charge rate $\lambda_{\mathrm{eff}_1} + \lambda_{\mathrm{eff}_2} = 2220 \pm 260\ \mathrm{s}^{-1}$ in good agreement with the dedicated measurement of the charge fluctuations on each test mass shown in Table I. The charge noise observed in these two measurements, separated by 60 days, is stationary to better than 10% and shows no measurable departure from a pure Poissonian behavior.

In order to calculate Δ_x and the required compensation voltages, dF/dq was determined from Δg using four charge steps of ∼0.6 pC. The charge was measured throughout with $V_{\mathrm{MOD}} = 50$ mV and $f_{\mathrm{MOD}} = 5$ mHz. Figure 2 shows q and Δg as a function of time through one of these measurements. The charge steps were repeated with V_{COMP} of -20, 0, $+20$ mV and the dependence of dF/dq on V_{COMP} confirms our electrostatic model to better than 2%. Two measurements on each GRS were made 45 days apart, the second with Δ_x on TM 1 compensated within 3 mV. At this level, the contribution to $S_{\Delta g}^{1/2}$ from random charging is 0.2 $\mathrm{fm\,s^{-2}\,Hz^{-1/2}}$ at 0.1 mHz. A further three measurements were made seven months later, the first on TM 1 and a final measurement on each TM after reducing the temperature of the sensor from ∼22 to ∼11 °C.

The calculated values for Δ_x, corrected for applied compensation, are given in Table II and plotted in Fig. 2 against the system pumping time. We note that the rotational stray-field imbalance, Δ_ϕ and Δ_η, that couple TM charge into torque in analogous fashion to Eq. (1), have

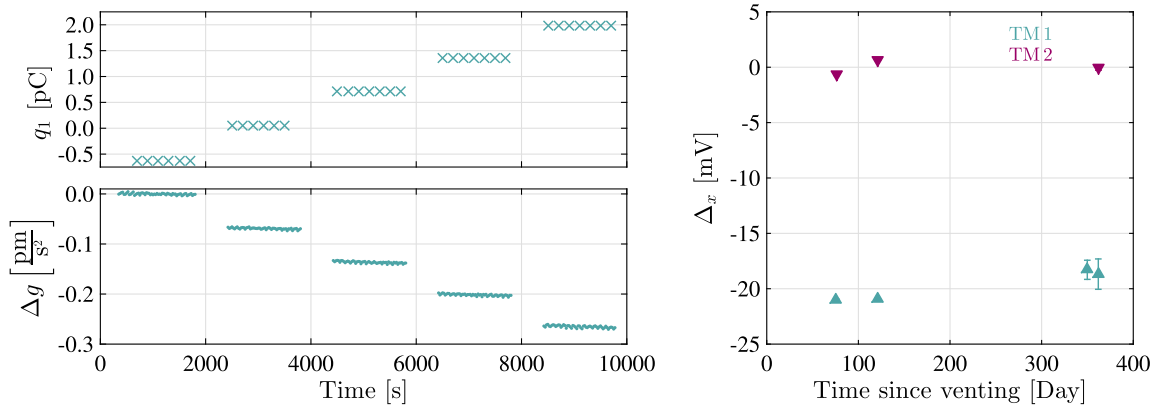

FIG. 2. Estimation of Δ_x. Left: Time series of charge steps in q_1 (cross) and Δg (dot) for measurement on TM 1 on day 110 of 2016 with no applied compensation. Data during UV Illumination periods lasting ∼100 s have been removed. Right: Seven measurements of uncompensated Δ_x on TM 1 (upward triangle) and TM 2 (downward triangle), plotted against the time elapsed since opening the vacuum chambers containing the GRS to space.

TABLE II. Estimates of uncompensated Δ_x.

Date	Δ_{x1}	Δ_{x2}	
2016-110	-21.02 ± 0.07	-0.67 ± 0.07	mV
2016-155	-20.93 ± 0.04	$+0.66 \pm 0.03$	mV
2017-018	-18.3 ± 0.9	⋯	mV
2017-030	-18.7 ± 1.4	-0.1 ± 0.2	mV

been measured in the same experiments to be roughly −32 and +36 mV for TM 1 and +119 and +84 mV for TM 2. When considered with the uncompensated values measured for Δ_x, roughly −20 mV and 0 mV for TM 1 and TM 2, the stray fields in the GRS would seem to be similar in magnitude to those observed in various measurements on GRS prototype hardware on ground [2,30,31]. Small but significant changes in Δ_x are observed for the two TMs, consistent with drifts of slightly less than mV/month, roughly an order of magnitude below typical drift values observed, for a limited number of samples, on ground [2,32]. This suggests that only very infrequent repetition of the measurement and compensation scheme will be necessary in LISA to keep acceleration noise from TM charge fluctuations below a tolerable level.

The spectral density of stray-voltage fluctuations was measured by increasing the test-mass charge and using a similar method to that used to observe the charge-noise effect on $S_{\Delta g}^{1/2}$. Figure 3 shows two measurements of the ASD of Δg, the first, over nearly two days (average of six, overlapping, 40 000-s windows), with normal levels of TM potential: $\langle V_{\mathrm{TM1}} \rangle = -16$ mV and $\langle V_{\mathrm{TM2}} \rangle = -24$ mV, followed within a day by a measurement of just over two days (eight, 40 000-s windows) at $\langle V_{\mathrm{TM1}} \rangle = -1066$ mV and $\langle V_{\mathrm{TM2}} \rangle = -1058$ mV. Fitting a polynomial to the excess in the PSD of Δg proportional to V_{TM}^2 of the form $S_{\Delta g} = [A^2(1\ \mathrm{mHz}/f)^2 + B^2(1\ \mathrm{mHz}/f)](V_{\mathrm{TM}}/1\ \mathrm{V})^2$, we find $A = 3.5 \pm 0.7\ \mathrm{fm\,s^{-2}\,Hz^{-1/2}}$ and $B = 6.4 \pm 0.5\ \mathrm{fm\,s^{-2}\,Hz^{-1/2}}$. This converts to an ASD of the

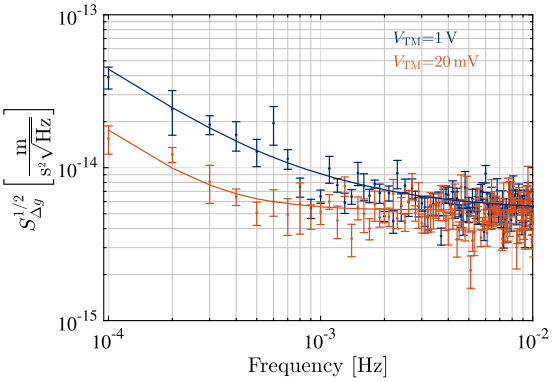

FIG. 3. Spectral density of consecutive measurements of Δg with $V_{\mathrm{TM}} = 1$ V (dark-blue indicators) and 20 mV (red indicators). A combined fit to the background and V_{TM}-dependent component is shown with continuous curves (reduced $\chi^2 = 1.1$).

fluctuations in Δ_x of $34 \pm 2\ \mu\mathrm{V\ Hz^{-1/2}}$ at 1 mHz and $190 \pm 30\ \mu\mathrm{V\,Hz^{-1/2}}$ at 0.1 mHz. Thus, the measured fluctuations in Δ_x are clearly resolved and are consistent with the upper limits placed for a GRS prototype on ground [2]. They are also consistent with ground measurements of the low-frequency actuation-circuitry voltage noise, which is indistinguishable from stray surface potential fluctuations in our acceleration noise measurement.

Throughout the majority of the operational phase of the mission, V_{TM} has been controlled within ±80 mV of zero by discharging under UV illumination during weekly or fortnightly interruptions to science measurements for orbital correction. The rms V_{TM} in a two-week measurement period such as that described in [9] is typically <40 mV and the contribution to $S_{\Delta g}^{1/2}$ at 0.1 mHz is $1.6 \pm 0.2\ \mathrm{fm\,s^{-2}\,Hz^{-1/2}}$.

Conclusions.—We have presented the most sensitive measurements of charge-related electrostatic forces on free-falling test masses relevant for sensitive gravitational experiments in space. Technology and mitigation methods developed for minimizing these forces on test masses in capacitive position sensors have been demonstrated and are directly transferable to LISA. Their contribution to the acceleration noise of individual test masses has been reduced to a level of roughly $1\ \mathrm{fm\,s^{-2}\,Hz^{-1/2}}$ at 0.1 mHz, compatible with the budgeted allocation for electrostatic forces contributing to the total acceleration noise in LISA [7].

The optimal method of test-mass charge control in a future space-based GW observatory will minimize the disruption to observations and the total contribution to acceleration noise. A continuous UV discharge scheme trades additional random-charging noise for a reduced coupling between V_{TM} and fluctuating stray potentials. Since the latter dominates the charge-related noise in the periodic discharge scenario described in this Letter by a factor of nearly 50 in power, it is likely some improvement can be obtained with a continuous scheme. This will be studied in a future experiment.

The methods and technology described here can enable a new generation of instrumentation for gravity-gradiometry and fundamental physics with improved performance in the milli-Hz regime.

This work has been made possible by the LISA Pathfinder mission, which is part of the space-science program of the European Space Agency. The French contribution has been supported by CNES (Accord Specific de Projet No. CNES 1316634/CNRS 103747), the CNRS, the Observatoire de Paris and the University Paris-Diderot. E. P. and H. I. would also like to acknowledge the financial support of the UnivEarthS Labex program at Sorbonne Paris Cit (Grants No. ANR-10-LABX-0023 and No. ANR-11-IDEX-0005-02). The Albert-Einstein-Institut acknowledges the support of the

German Space Agency, DLR. The work is supported by the Federal Ministry for Economic Affairs and Energy based on a resolution of the German Bundestag (Grants No. FKZ 50OQ0501 and No. FKZ 50OQ1601). The Italian contribution has been supported by Agenzia Spaziale Italiana and Instituto Nazionale di Fisica Nucleare. The Spanish contribution has been supported by Contracts No. AYA2010-15709 (MICINN), No. ESP2013-47637-P, and No. ESP2015-67234-P (MINECO). M. N. acknowledges support from Fundacion General CSIC Programa ComFuturo). F. R. acknowledges support from a Formacin de Personal Investigador (MINECO) contract. The Swiss contribution acknowledges the support of the Swiss Space Office (SSO) via the PRODEX Programme of ESA. L. F. acknowledges the support of the Swiss National Science Foundation. The UK groups wish to acknowledge support from the United Kingdom Space Agency (UKSA), the University of Glasgow, the University of Birmingham, Imperial College London, and the Scottish Universities Physics Alliance (SUPA). J. I. T. and J. S. acknowledge the support of the U.S. National Aeronautics and Space Administration (NASA).

*Corresponding author.
p.wass@imperial.ac.uk
†Deceased.
‡Present address: Physics and Instrumentation Department, ONERA, the French Aerospace Lab, 92320 Chatillon, France.

[1] D. N. A. Shaul, H. M. Araújo, G. K. Rochester, T. J. Sumner, and P. J. Wass, Evaluation of disturbances due to test mass charging for LISA, Classical Quantum Gravity **22**, S297 (2005).

[2] F. Antonucci, A. Cavalleri, R. Dolesi, M. Hueller, D. Nicolodi, H. B. Tu, S. Vitale, and W. J. Weber, Interaction between Stray Electrostatic Fields and a Charged Free-Falling Test Mass, Phys. Rev. Lett. **108**, 181101 (2012).

[3] D. V. Martynov, E. D. Hall, B. P. Abbott *et al.*, Sensitivity of the Advanced LIGO detectors at the beginning of gravitational wave astronomy, Phys. Rev. D **93**, 112004 (2016).

[4] T. J. Sumner, J. Anderson, J.-P. Blaser *et al.*, STEP (satellite test of the equivalence principle), Adv. Space Res. **39**, 254 (2007).

[5] S. Buchman and J. P. Turneaure, The effects of patch-potentials on the gravity probe B gyroscopes, Rev. Sci. Instrum. **82**, 074502 (2011).

[6] P. McNamara, S. Vitale, and K. Danzmann, LISA Pathfinder, Classical Quantum Gravity **25**, 114034 (2008).

[7] K. Danzmann *et al.*, Report No. ESA/SRE2011(2011)3, 2011.

[8] K. Danzmann *et al.*, LISA: Laser Interferometer Space Antenna, arXiv:1702.00786.

[9] M. Armano, H. Audley, G. Auger *et al.*, Sub-Femto-g Free Fall for Space-Based Gravitational Wave Observatories: LISA Pathfinder Results, Phys. Rev. Lett. **116**, 231101 (2016).

[10] R. Dolesi, D. Bortoluzzi, P. Bosetti *et al.*, Gravitational sensor for LISA and its technology demonstration mission, Classical Quantum Gravity **20**, S99 (2003).

[11] W. J. Weber, D. Bortoluzzi, C. Carbone *et al.*, Position sensors for flight testing of LISA drag-free control, Proc. SPIE Int. Soc. Opt. Eng. **4856**, 31 (2003).

[12] C. C. Speake, Forces and force gradients due to patch fields and contact-potential differences, Classical Quantum Gravity **13**, A291 (1996).

[13] P. Touboul, B. Foulon, and E. Willemenot, Electrostatic space accelerometers for present and future missions, Acta Astronaut. **45**, 605 (1999).

[14] B. Lenoir, A. Lévy, B. Foulon, B. Lamine, B. Christophe, and S. Reynaud, Electrostatic accelerometer with bias rejection for gravitation and Solar System physics, Adv. Space Res. **48**, 1248 (2011).

[15] J. Bergé, B. Christophe, and B. Foulon, GOCE accelerometers data revisited: Stability and detector noise, in *Proceedings of ESA Living Planet Symposium, 2013, Edinburgh, UK*, edited by L. Ouwehand (ESA Communications, Noordwijk, Netherlands, 2013), Vol. SP-772, p. 29.

[16] G. Heinzel, C. Braxmaier, R. Schilling, A. Rüdiger, D. Robertson, M. te Plate, V. Wand, K. Arai, U. Johann, and K. Danzmann, Interferometry for the LISA technology package (LTP) aboard SMART-2, Classical Quantum Gravity **20**, S153 (2003).

[17] G. Heinzel, V. Wand, A. García *et al.*, The LTP interferometer and phasemeter, Classical Quantum Gravity **21**, S581 (2004).

[18] H. Audley, K. Danzmann, A. García-Marín *et al.*, The LISA Pathfinder interferometry hardware and system testing, Classical Quantum Gravity **28**, 094003 (2011).

[19] D. Mance, Ph.D. thesis, University of Split, 2012.

[20] Y. Jafry, T. J. Sumner, and S. Buchman, Electrostatic charging of space-borne test bodies used in precision experiments, Classical Quantum Gravity **13**, A97 (1996).

[21] H. M. Araújo, P. J. Wass, D. N. A. Shaul, G. Rochester, and T. J. Sumner, Detailed calculation of test-mass charging in the LISA mission, Astropart. Phys. **22**, 451 (2005).

[22] P. J. Wass, H. M. Araújo, D. N. A. Shaul, and T. J. Sumner, Test-mass charging simulations for the LISA Pathfinder mission, Classical Quantum Gravity **22**, S311 (2005).

[23] C. Grimani, H. Vocca, G. Bagni, L. Marconi, R. Stanga, F. Vetrano, A. Viceré, P. Amico, L. Gammaitoni, and F. Marchesoni, LISA test-mass charging process due to cosmic-ray nuclei and electrons, Classical Quantum Gravity **22**, S327 (2005).

[24] C. Grimani, M. Fabi, A. Lobo, I. Mateos, and D. Telloni, LISA Pathfinder test-mass charging during galactic cosmic-ray flux short-term variations, Classical Quantum Gravity **32**, 035001 (2015).

[25] M. Schulte, G. K. Rochester, D. N. A. Shaul, T. J. Sumner, C. Trenkel, and P. J. Wass, The charge-management system on LISA-Pathfinder: Status & outlook for LISA, AIP Conf. Proc. **873**, 165 (2006).

[26] S. Buchman, T. Quinn, G. M. Keiser, D. Gill, and T. J. Sumner, Charge measurement and control for the Gravity Probe B gyroscopes, Rev. Sci. Instrum. **66**, 120 (1995).

[27] H. M. Araújo, A. Howard, D. Davidge, and T. J. Sumner, Charging of isolated proof masses in satellite experiments

such as LISA, Proc. SPIE Int. Soc. Opt. Eng. **4856**, 55 (2003).

[28] P. J. Wass, L. Carbone, A. Cavalleri *et al.*, Testing of the UV discharge system for LISA Pathfinder, AIP Conf. Proc. **873**, 220 (2006).

[29] S. E. Pollack, M. D. Turner, and S. Schlamminger, Charge management for gravitational-wave observatories using UV LEDs, Phys. Rev. D **81**, 021101 (2010).

[30] L. Carbone, A. Cavalleri, R. Dolesi, C. D. Hoyle, M. Hueller, S. Vitale, and W. J. Weber, Achieving Geodetic Motion for LISA Test Masses: Ground Testing Results, Phys. Rev. Lett. **91**, 151101 (2003).

[31] W. J. Weber, L. Carbone, A. Cavalleri, R. Dolesi, C. D. Hoyle, M. Hueller, and S. Vitale, Possibilities for measurement and compensation of stray DC electric fields acting on drag-free test masses, Adv. Space Res. **39**, 213 (2007).

[32] S. E. Pollack, S. Schlamminger, and J. H. Gundlach, Temporal Extent of Surface Potentials between Closely Spaced Metals, Phys. Rev. Lett. **101**, 071101 (2008).